Millennial Climate Variability: Is There a Tidal Connection?

WALTER MUNK AND MATTHEW DZIECIUCH

Scripps Institution of Oceanography, University of California, San Diego, La Jolla, California

STEVEN JAYNE

CIRES and Department of Physics, University of Colorado, Boulder, Colorado

ABSTRACT

Orbital forcing has long been the subject of two quite separate communities: the tide community is concerned with the relatively rapid gravitational forces (periods up to 18.6 yr) and the climate community with the long-period Milankovitch insolation terms (exceeding 20 000 yr). The wide gap notwithstanding, the two subjects have much in common. Keeling and Whorf have proposed that the millennial climate variability is associated with high-frequency tidal forcing extending into the 10-octave gap by some nonlinear process. Here, the authors distinguish between two quite distinct processes for generating low frequencies: (i) the ''traditional'' analogy with eclipse cycles associated with near coincidence of the appropriate orbital alignment of the Sun, the Moon, and Earth, and (ii) sum and differences of tidal frequencies and their harmonics producing low beat frequencies. The first process is associated with long time intervals between extreme tides, but the events are of short duration and only marginally higher than conventional high tides. With proper nonlinearities, (ii) can lead to low-frequency tidal forcing. A few candidate frequencies in the centurial and millennial band are found, which prominently include the Keeling and Whorf at 1795 yr. This is confirmed by a numerical experiment with a computer-generated tidal time series of 275 000 yr. Tidal forcing is very weak and an unlikely candidate for millennial variability; the Keeling and Whorf proposal is considered as the most likely among unlikely candidates.

1. Introduction

Evidence for climatic variability on a millennial scale has been found in ice cores and deep sea sediments (see Bond et al. 1997, 1999; Alley and Clark 1999 for recent reviews). Prominent layers of ice-rafted debris in North Atlantic sediment cores, presumably associated with ocean surface cooling, show that ''. . . the 1–2 kyr cycle is a persistent feature of climate,'' with 0.55 ± 0.15 cycles per kiloyear (cpky) (1400–2500 yr) as representative of the millennial climate spectrum (Bond et al. 1999; Fig. 1). Grootes and Stuiver (1997) find a broad peak at the 1500-yr period in the spectrum of $\delta^{18}O$ data for the Greenland Ice Sheet. With regard to the generating mechanism, suggestions include solar forcing, internal dynamics of the ocean–atmosphere system and harmonics of the Milankovitch orbital frequencies; according to Bond et al. ''none of those alternatives is supported thus far by particularly compelling evidence.''

Yet a different hypothesis has been proposed by Keeling and Whorf (hereafter KW; 1997, 2000); KW suggest that the millennial variability is related to extreme oceanic tides associated with orbital coincidences reoccurring at certain repeat periods; further, that strong tidal forcing causes cooling of the sea surface by increased vertical mixing. The KW proposal resembles a hypothesis put forward by Pettersson (1914, 1930). This again is based on orbital coincidences (including 1500 yr among other periods), and derives from Pettersson's discovery of a scattering of surface tides into giant internal tides (and eventually turbulent mixing) at the sills of Scandinavian fjords.

There are many options concerning the generation of millennial variability (Fig. 2). First there is the question of orbital forcing versus an *internal* variability inherent in ocean–atmosphere dynamics. In the former case we expect the response to be characterized by a narrow spectral *line,* in the latter case by a broad spectral *band* (as observed). With regard to orbital forcing, we distinguish between the Milankovitch terms and what are usually called the tide-producing forces; the former have periods much longer, and the latter periods much shorter, then the millennial variability. The KW proposal is for nonlinear interaction between the high-frequency tidal constituents producing low-frequency forcing.

Corresponding author address: Prof. Walter Munk, Institute of Geophysics and Planetary Physics, Scripps Institution of Oceanography, University of California, San Diego, Mail Code 0225, La Jolla, CA 92093-0225.
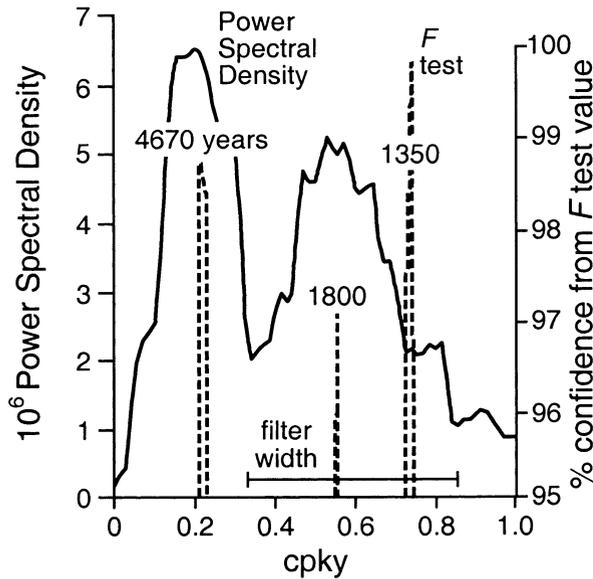E-mail: wmunk@ucsd.edu

FIG. 2. Sketch of some of the issues involved in the generation of millennial climate variability.

associated with the acceleration of the lunar orbit due to tidal friction.

2. External forcing versus internal variability

The most fundamental question is whether the millennial variability is associated with internal processes inherent in ocean–atmosphere dynamics, or whether it is externally forced by radiational–gravitational fluctuations inherent in the solar system. ENSO and the North Atlantic oscillation are considered to be of the former type, and much effort has gone into understanding the internal dynamics. Among external forcing we need to distinguish between orbital forcing, and the possible effect of a variable solar radiation.

A distinction between orbital forcing (whether Milankovitch or tidal) and internal variability can be made on the basis of bandwidth of the response. Orbital forcing is at precise frequencies (spectral "lines"); the frequencies are given to eight significant figures and meaningful predictions (and hindcasts) can be carried out for 10 million years. (But lines are not infinitely narrow because of tidal friction, planetary perturbations, etc.) Internal ocean–atmosphere processes are broadband, and predictions are limited to a few cycles. The experimental evidence suggests that the millennial variability is spread over a band (Fig. 1). But the evidence is not conclusive. Lines are spread into bands by poor resolution and sampling error, and bands can be collapsed into lines by "overtuning" (see Muller and MacDonald 2000). A comparison of the relative contributions to the record variance of the spectral lines and the continuum requires a comparison of line *heights* and continuum *area* (see appendix A for a discussion).

One can expect both lines and a continuum in the spectrum of any geophysical time series. At tidal frequencies (Fig. 3) the situation is as follows: for frequencies above 1 cycle per year (cpy) the line spectrum dominates over the continuum "noise," (the strategy of tidal analysis until the 1960s was consistent with the
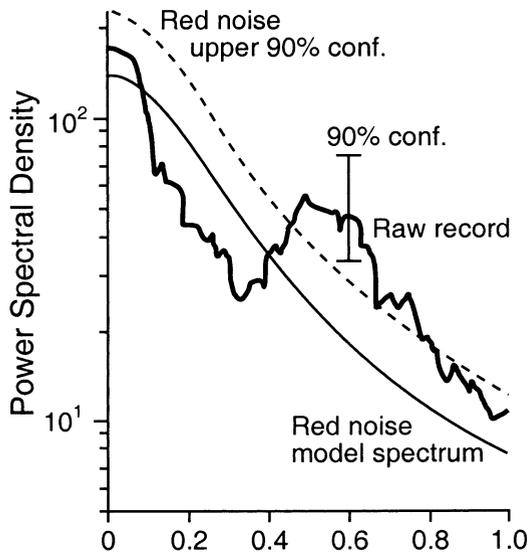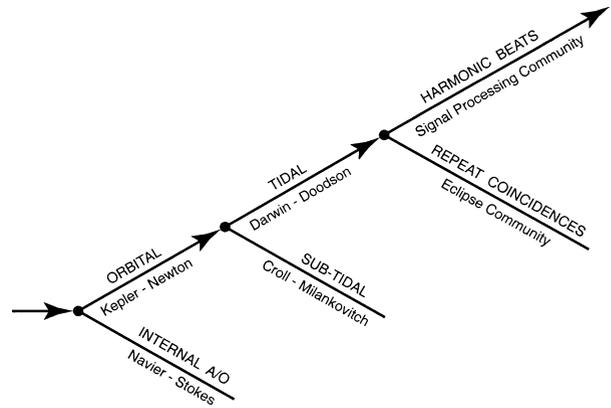
FIG. 1. Power spectra of hematite-stained grains from deep sea sediment cores in the subpolar North Atlantic. The time series spanning 80 kyr is a sensitive measure of ice-rafting episodes associated with ocean surface cooling [Bond et al. 1997 (bottom), 1999 (top)].

Here we must distinguish between two distinct processes leading to low-frequency generation: *repeat coincidence* (RC) of orbital parameters, and *harmonic beats* (HB). A tidal forcing at 0.56 cpky (1795 yr) resulting from an interaction between yearly, lunar perigean, and lunar nodal forcing has been proposed by KW. We examine the set of possible nonlinear interactions and find the KW frequency to be unique among harmonic beat frequencies. This is confirmed by a numerical experiment subjecting a 275 000-yr tidal time series to various nonlinearities. Some of the harmonic beat frequencies in the cpky range have a secular change
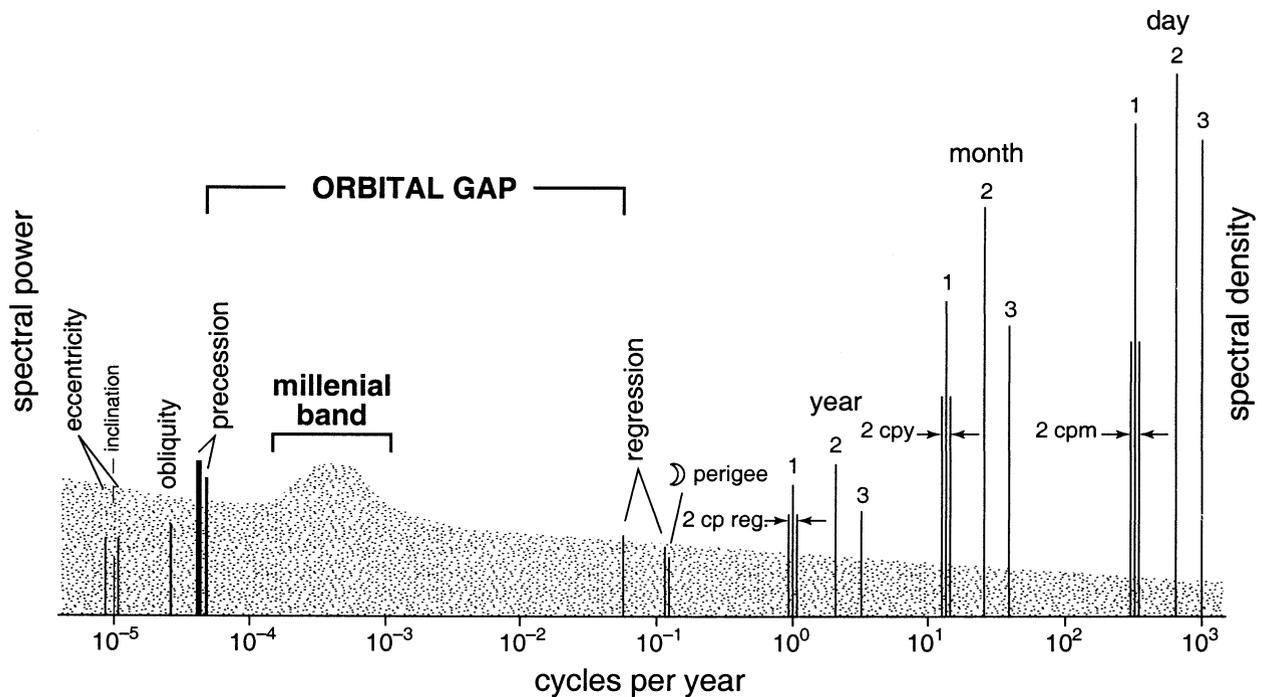
FIG. 3. Cartoon of climate variability. Vertical lines represent the combined gravitational–radiational forcing at various orbital frequencies. There is a gap of orbital forcing between periods of 18.6 and 20 000 yr. The dotted band underlying the climate line spectrum designates the continuous spectrum, with the millennial band indicated. The line spectrum and the continuum have different dimensions, both drawn to arbitrary scale. The relative heights of the tidal lines (right) show a gravitational bias; for radiational forcing the annual lines are enhanced.

assumption of an infinite signal-to-noise ratio). The detection of the intertidal continuum had to await the development of modern computers (Munk and Bullard 1963; Munk and Cartwright 1966). Below 1 cpy the continuum takes over, and very long records are required to even detect the tidal lines above the continuum. So both the lines and the continuum are essential components of the spectrum at tidal frequencies. With regard to the climate spectrum, there has been remarkable success in identifying the Milankovitch orbital lines in the sedimentary record. But lines are the more appealing manifestation of variability, and the evidence is still out on what fraction of the climate variance is associated with the intertidal continuum relative to that in the line spectrum.

3. Orbital forcing

a. Milankovitch versus Darwin–Doodson

Figure 3 is a very crude attempt to pull together the work of two distinct communities: climate (left) and tides (right). The principal tidal lines are to the right and clustered about five frequency ranges: cycles per day (cpd), per month (cpm), per year (cpy), per lunar perigee (8.8 yr), and regression (18.6 yr). Higher harmonics of principal frequencies (such as 3, 4, . . . cpm) diminish in amplitude like ξ^3, ξ^4, where ξ is the parallax (Earth radius/distance, 1/59.6 for the Moon, 1/23 400

for the Sun). Multiples are associated with Kepler–Newton nonlinearity: cpm splitting of the cpd lines, cpy splitting of cpm lines, etc. The cpm fine structure of the cpd lines is further split into a cpy hyperfine structure (not shown), etc.

To the left are the so-called Milankovitch (1941) terms of orbital motion. These are associated with perturbations in the Earth–Moon–Sun system by other planets. The principal terms are precession (19 and 23 ky), obliquity (41 ky), and eccentricity (95, 100, 213, 413 kyr) [or inclination (100 kyr), see Berger (1999); Muller and MacDonald (2000)]. Here again Kepler–Newton nonlinearity leads to a fine structure of sum and difference frequencies.

Note the 1:1000 ratio between the longest "traditional" tide period of 18.6 yr and the shortest Milankovitch period of 20 000 yr, defining the boundaries to an "orbital gap." Forcing within the gap might be attributed to high harmonics of the Kepler–Newton orbital nonlinearities in the Milankovitch terms, or low frequencies associated with Navier–Stokes nonlinearities in the tidal terms. The latter alternative has been chosen by KW.

Starting with Lord Kelvin, the traditional analysis of tide records by Darwin (Sir George, son of Charles) was entirely in the frequency domain. Fitting the data by a few dozen parameters as a basis for tide prediction was one of the success stories of the late nineteenth century.

By 1921 the Doodson expansion had led to 358 terms, most of them buried in the continuum noise (Doodson 1921). Here we shall use a direct integration scheme in the time domain (far more frugal in parameter space) developed by Cartwright (Munk and Cartwright 1966; Cartwright and Tayler 1971; Cartwright and Edden 1973). (We note that Doodson and Cartwright formally include the perihelion period of 20.94 ky on the other side of the "gap.")

The original Milankovitch formulation was entirely in the frequency domain, leading up to 47 terms in the 1970s. Fitting the sedimentary and ice records by the Milankovitch frequencies is one of the success stories of the late twentieth century. But for very long time-scales subject to planetary perturbations a direct inte-gration scheme pioneered by Laskar (1986) and Quinn et al. (1991) has led to a convenient presentation in the time domain (see also Laskar 1999; Muller and Mac-Donald 2000).

The transition in both the tidal and the climate anal-yses from the frequency to the time domain is an in-evitable result of dealing with "almost (but not quite) periodic functions," associated with weak perturbations. Records "shorter" than the perturbation timescale (100 kyr) are conveniently analyzed in the frequency domain, for longer records a comparison between orbital forcing and climate response can be conveniently performed in the time domain (Shackleton et al. 1999).

b. Insolation versus gravity

The ordinate in Fig. 3 has not been specified. For the Milankovitch forcing the ordinate is insolation (radia-tion in W m^{-2} impinging on the upper atmosphere). For the tidal forcing it is the gravity potential V, or equiv-alently the equilibrium height $V g^{-1}$. Comparing inso-lation to tidal height may seem like comparing apples and oranges. But this is not so.

Even for a traditional tide prediction some radiational terms need to be included to give sensible results. For example, the annual and semiannual tides are dominated by nongravitational effects such as the thermal expan-sion of the water column and, more important, land-and-sea breeze and other wind forcing. The "response method" of tide prediction introduces a "radiational tide potential" (closely related to insolation) in addition to the traditional gravity potential (Munk and Cartwright 1966). In this sense there is a continuity from the short-est semidiurnal tide to the longest Milankovitch orbital forcing. Given the solar mass and radiance, the response of sea level to gravitational and radiational forcing is surprisingly competitive (appendix B).

A quite different connection between tides and cli-mate is associated with a thermal response to gravita-tional forcing. This is the route taken by KW (2000): ". . . variations in the strength of oceanic tides cause periodic cooling of surface ocean water by modulating the intensity of vertical mixing that brings to the surface

colder water from below," in line with Garrett's (1979) suggestion of an 18.6-yr cycle in surface temperature. [But a "bidecadal" climate signal appears to be an ir-regular long-term ENSO cycle and not of tidal origin (Ghil and Vautard 1991; Mann and Park 1994; but see Cerveny and Shaffer 2001).] A more likely scenario makes the connection in terms of the poleward heat transport (rather than surface temperature) as the per-tinent climate variable. Interior mixing powered by tides significantly modulates the meridional overturning cir-culation and thus the equator-to-pole heat transport (Munk and Wunsch 1998). The scenario involves high nonlinearities (mixing by internal wave breaking) on a millennial timescale (bottom water renewal), but we have made no attempt at a quantitative analysis.

4. Nonlinear generation of low frequencies

We now explore tidal forcing in the millennial gap at frequencies well below the frequencies of the fun-damental tidal constituents. This is the main topic of Keeling and Whorf (1997, 2000).

Times of extreme tide-producing forces requires the following three conditions to occur nearly simultaneous-ly: (i) Earth at perihelion, (ii) longitude of the Moon's perigee near perihelion or aphelion, and (iii) longitude of the Moon's node near perihelion or aphelion. Pet-tersson (1930) refers to "parallactic tides" as represen-tative of a near overlap; they are the subject of a mono-graph by Wood (1986) who refers to them as the "peri-gean tides." An example going back to the classics is the *metonic* cycle of 19 tropical years, which is very close to 254 tropical months (19.0002 tropical years). For even longer intervals one can find even closer over-laps and more extreme tides. These perigean tides are characterized by being of short duration (a fraction of a tidal cycle) and of only slightly greater amplitude than ordinary high tides.

Perigean tides are appropriate if we wish to predict spilling over a sea wall; the prediction of eclipses are of this type since they involve the precise alignment of several orbital parameters. And this would be the proper metric for climate variability if, for example, the loss of radiation during solar eclipses were a significant fac-tor in the radiation balance of the Earth.

A different physics is based on the beat frequencies between the harmonics of the tidal frequencies. Some of the harmonics are densely packed with opportunities for small difference frequencies, as will be shown. The generation of sum and difference frequencies is the fa-miliar tool of the signal processing community.

We shall use the terms "repeat coincidence (RC)" and "harmonic beats (HB)" to refer to the two foregoing procedures. Both procedures are based on a near com-mensurability of tidal frequencies or their harmonics, but are otherwise quite distinct. Here RC is the appro-priate language for eclipse problems; we believe that HB is the appropriate formalism for considering tidal

forcing of millennial climate variability (if indeed there is significant tidal forcing).

Pettersson (1930) ascribes climate variability to a number of coincidences such as the metonic cycle and longer periods "... up to 1850 years, the longest that I have been able to find" but gives no indication of how he came up with 1850 years. Keeling and Whorf (1997) speak of the "... slight degree of misalignment and departures from the closest approach of the Earth with the Moon and Sun at the time of extreme tide raising forces." Using such RC language to discuss climate problems confuses the issue. There is further confusion in that the 1795-yr period proposed by KW is actually of the HB type.

We now develop the two formalisms quantitatively (the reader already persuaded may wish to go directly to section 6).

a. Harmonic beats and repeat coincidences

We start with a greatly simplified problem of two frequencies f_a and f_b:

$$x(t) = \frac{1}{2}\cos(2\pi f_a t) + \frac{1}{2}\cos(2\pi f_b t)$$

$$= \cos(2\pi f_c t)\cos(2\pi f_m t), \qquad (4.1)$$

where $f_c = \frac{1}{2}(f_a + f_b)$ and $f_m = \frac{1}{2}(f_a - f_b)$ are the carrier and modulation frequencies.

HB: Generate the n_ath harmonic of f_a and the n_bth harmonic of f_b and form the difference frequency

$$\delta f = n_a f_a - n_b f_b \qquad (4.2)$$

with n_a and n_b so chosen that $|\delta f|$ is small compared to f_a and f_b.

RC: Let the two sinusoids be exactly in phase at time 0 with perfect constructive interference, $x(0) = 1$ say. Events of near-perfect constructive interference occurs at intervals T when an integer number n_a of periods f_b^{-1} nearly coincides with an integer number n_b of periods f_b^{-1}:

$$T_a \approx T_b, \qquad T_a = n_a f_b^{-1}, \qquad T_b = n_b f_a^{-1} \qquad (4.3)$$

with

$$\delta T = n_a f_b^{-1} - n_b f_b^{-1} \qquad (4.4)$$

a measure of departure from perfect overlap. The associated RC frequencies $f_a/n_b \approx f_b/n_a$ are subharmonics of the initial frequency pair. The repeat periods become successively longer as all but the highest events are excluded.

We rationalize f_b/f_a with integers n_a and n_b such that the *incommensurability parameter* is given by

$$\epsilon \equiv |f_a/f_b - n_b/n_a| \ll 1. \qquad (4.5)$$

It follows that

$$\delta f = \epsilon n_a f_b, \qquad \delta T = \epsilon n_a f_b^{-1} \qquad (4.6)$$

so that both HB and RC both require $\epsilon \to 0$ to achieve low frequencies and high coincidence, respectively.

Let $T_{RC} = \frac{1}{2}(T_a + T_b)$ designate the intervals between constructive interference events. These occur at times when the carrier oscillation $\cos(2\pi f_c t)$ in Eq. (4.1) is very near unity, or

$$f_c t = 0, 1, 2, \ldots, k,$$

where k measures time in units of carrier cycles. At these times the modulation amplitude is $\cos(2\pi f_m t)$, with

$$f_m t = f_c t \frac{f_m}{f_c} = k\frac{(f_a/f_b) - 1}{(f_a/f_b) + 1} = k\frac{(n_b/n_a) + \epsilon - 1}{(n_b/n_a) + \epsilon + 1}$$

$$= k\frac{n_b - n_a}{n_b + n_a}\left(1 + \frac{2\epsilon n_a^2}{n_b^2 - n_a^2}\right) \qquad (4.7)$$

to order ϵ. Suppose

$$k = \frac{n_b + n_a}{n_b - n_a}l, \qquad l = 0, \pm 1, \pm 2, \ldots$$

so that $f_m t = \ell + $ order ϵ. For $\epsilon = 0$ the carrier and modulation peaks overlap with perfect constructive interference, $x = 1$. In general, the interference maximum is given by

$$\cos\left[2\pi l\left(1 + \frac{2\epsilon n_a^2}{n_b^2 - n_a^2}\right)\right] = \cos\left(\frac{4\pi\epsilon l n_a^2}{n_b^2 - n_a^2}\right)$$

$$= 1 - \frac{1}{2}\{\ \}^2 + \cdots. \qquad (4.8)$$

Thus δf and δT are both of order ϵ, whereas the amplitude loss relative to perfect constructive interference is of the order of ϵ^2.

Nearly commensurate frequencies ($\epsilon \to 0$) are prerequisite for both HB and RC events. Small integers n favor HB events, large integers make sense only for RC. HB events are of low frequency $\delta f \approx \epsilon n f$ and long duration [order $(\delta f)^{-1}$]. For RC events ϵ enters as an amplitude parameter: the *defect* (relative to perfect constructive interference) is of order ϵ^2. Frequencies are of order f/n and remain finite as $\epsilon \to 0$; durations are short, a fraction of f^{-1}.

The relative success of HB versus RC in producing low frequencies is measured by the product

$$\delta f T_a = \epsilon n_a^2, \qquad T_a > T_b, \qquad n_a > n_b. \qquad (4.9)$$

Thus, RC events with large n_a (such as the Saros and Metonic cycles) even though nearly commensurate ($\epsilon \ll 1$) are not associated with low HB frequencies.

b. Squaring, cubing, ... and other powers

Returning to (4.1), a squaring device $x^2(t)$ generates the five frequencies

$$0, \qquad f_a - f_b, \qquad 2f_a, \qquad f_a + f_b, \qquad 2f_b$$

including the important difference term $f_a - f_b = 2f_m$ of low (but nonzero) frequency. Cubing yields the difference frequencies $f_a - 2f_b$ and $2f_a - f_b$. Let $n = 0, \pm 1, \pm 2, \ldots$ For two or more frequencies, $x^p(t)$ generates the sum and difference frequencies

$$n_a f_a + n_b f_b + n_c f_c + \cdots,$$

$$|n_a| + |n_b| + |n_c| + \cdots$$

$$= p, p - 2, \ldots, 0 \text{ or } 1 \qquad (4.10)$$

for p even or odd. With suitable nonlinearities, all possible integer sums of harmonics are generated.

c. Clipping

Another nonlinear operation is

$$C_q(x) = \begin{cases} q & \text{for } x < q, \\ x & \text{for } x \geq q, \end{cases} \qquad (4.11)$$

with $x_{\min} < x < x_{\max}$. The function $x(t)$ is unchanged for $q < x_{\min}$. "Soft clipping" $q = x_{\min} + \epsilon$ fills the troughs and forms discontinuities in dx/dt. "Hard clipping" $q = x_{\max} - \epsilon$ results in intermittent pulses at high tide. All clipping, soft and hard, forms harmonics. Severe hard clipping produces isolated RC events.

The two operations $x^p(t)$ and $C_q[x(t)]$ will be taken as examples for nonlinearity, not because of their relation to any specific climate processes, but because they are simple and offer some analytical guidance.

d. A numerical example

For specificity we take

$$f_a = 3.05, \qquad f_b = 5, \qquad f_a/f_b = 0.61,$$

and generate the integers n_a and n_b by evaluating (Wolfram 1999, section 3.1.3)

$$|n_b/n_a| = \Re\{\phi; \epsilon\}, \qquad (4.12)$$

where $\Re\{\phi; \epsilon\}$ is a rational number approximation to ϕ within tolerance ϵ. For example, $\Re\{f_a/f_b; 0.01\} = 3/5$, $n_a = 5$, $n_b = 3$, yielding an HB frequency $\delta f = n_a f_b \epsilon = 0.25$ and the RC frequencies $3.05/3 = 1.02$, $5/5 = 1$ (see $5f_a - 3f_b$ in the bottom panels of Fig. 3a). In order of decreasing ϵ, we have

$$\epsilon = 0.39, 0.11, 0.06, \ldots, 0.01, 0$$

$$\left|\frac{n_b}{n_a}\right| = \frac{1}{1}, \frac{1}{2}, \frac{2}{3}, \ldots, \frac{3}{5}, \frac{61}{100}$$

$$\delta f = 1.95, 1.1, 0.85, \ldots, 0.25, 0$$

$$\frac{1}{T_{RC}} = 3.8, 2.7, 1.6, \ldots, 1.01, 0.05$$

$$\delta T = -0.13, +0.72, -0.055, \ldots, +0.016, 0.$$

The repeat period of 20 time units is exact (frequen-

cies are commensurate) and clearly seen in the clipped spectrum. This requires severe clipping of an appropriately limited record portion. Taking $\epsilon = 0.01$, $f_a = 3.05$, $f_b = 5$, $f_m = 0.975$, $f_c = 4.025$, $n_a = 5$, $n_b = 3$, Eq. (4.7) gives event times $f_m t = \ell = -2, -1, 0, 1, 2$ in agreement with Fig. 4. For earlier and later times the amplitude drops below 0.9 in accordance with Eq. (4.8). There are high events at subsequent times, but these are shifted in phase and drop out from a harmonic analysis on a single time base. Within the interval $-2.5 < t < +2.5$ (Fig. 4b), soft clipping produces HB, severely hard clipping produces RC events.

5. The Saros cycle and other repeat coincidences

Table 1 lists the basic tidal constituents with some of the classic notation. The basic constituents can be combined into various *derived* constituents (Table 2). For specificity, we select two derived constituents, the nodical and the synodic months, for the interacting frequencies:

$$f_a = f_{21} = f_2 + f_5, \qquad f_b = f_{23} = f_2 - f_4 \quad (5.1)$$

and generate the integers n_a and n_b by evaluating $\Re\{f_b/f_a; \epsilon\}$ for decreasing ϵ (Table 3). The parameter $n\epsilon$ increases with n for small n, then decreases. The well-known Saros cycle of eclipses (Fig. 5) corresponds to $n_a = 223$, $n_b = 242$, with

$$T_a = 242 f_a^{-1} = 18.0300 \text{ yr},$$

$$T_b = 233 f_b^{-1} = 18.0301 \text{ yr}. \qquad (5.2)$$

Note the minimum in $n\epsilon$ for the Saros values, yielding $\delta T = 10^{-4}$ yr with no improvement in going to even higher n values.

The "metonic cycle," which governs the repetition of lunar phases, involves only two basic frequencies, the month and the year:

$$254/f_2 = 19.0002, \qquad 19/f_3 = 19 \qquad (5.3)$$

with $\delta T = 2 \times 10^{-4}$ yr. We remark that the metonic 19-yr period, the Saros 18-yr period, and the lunar regression period $f_5^{-1} = 18.61$ yr are quite independent though their periods are close.

Cartwright (1974) points to the near coincidence of 5 times the period of regression of lunar nodes with 10.5 times the period of lunar perigee (half integers are permitted)

$$5/f_5 = 93.1 \text{ yr}, \qquad 10.5/f_4 = 92.9 \text{ yr}, \quad (5.4)$$

giving rise to a 93-yr RC period with only moderate harmonics. We find many combinations $\{n_4, n_5\}$ such as $\{10, 21\}$, $\{19, 40\}$, $\{29, 61\}$, …producing rough multiples of 93 yr.

6. Keeling–Whorf harmonic beat frequency

From now on we are concerned only with HB frequencies as a possible source of climate variations. The
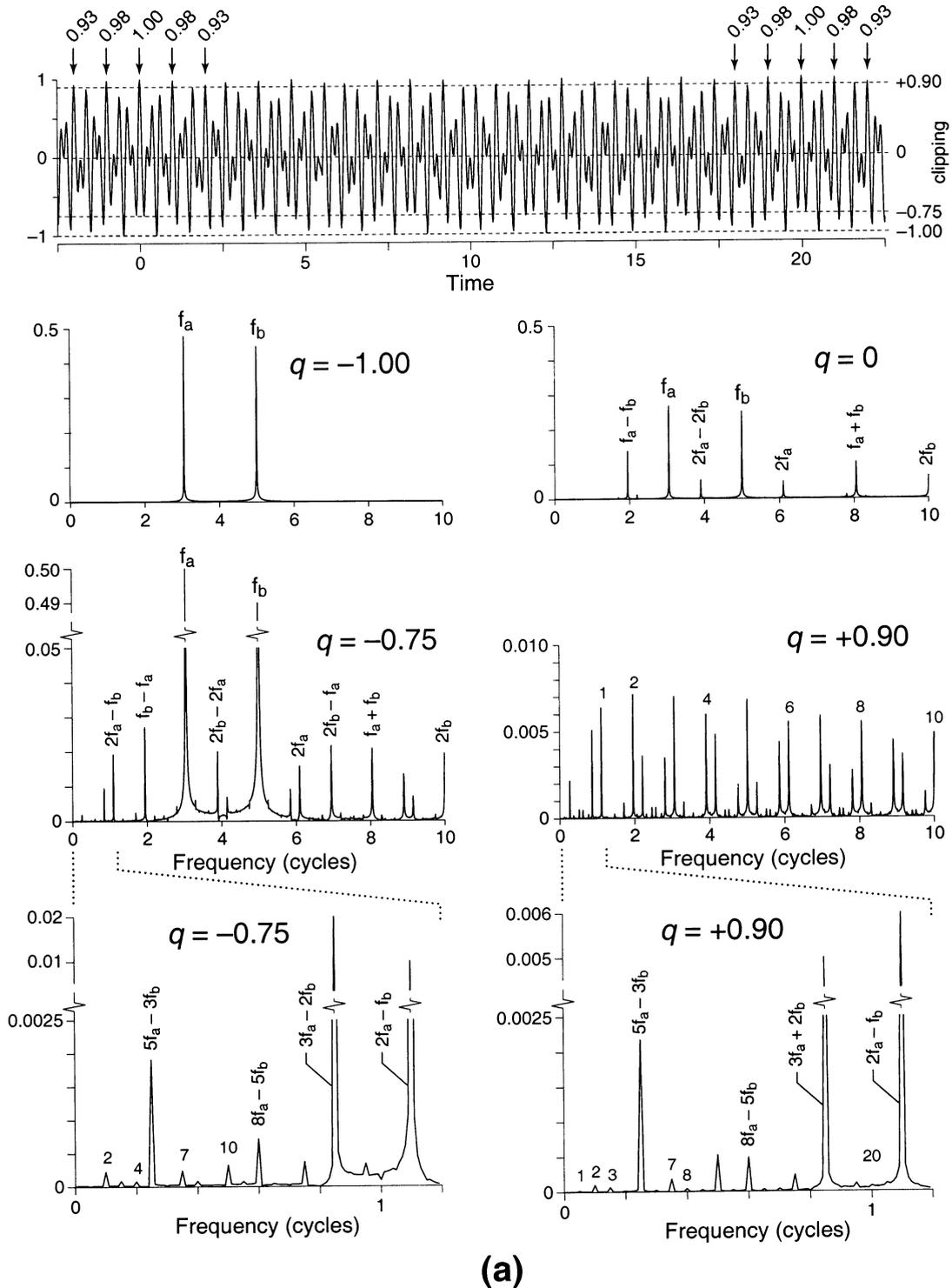
(a)

FIG. 4. An artificial example of the generation of HB and RC. Two sinusoids of amplitude 1/2 and frequencies f_a = 3.05 and f_b = 5 cycles per unit time produces an interference pattern that repeats in T = 20 time units for every 61 f_a-cycles and 100 f_b-cycles; there is also a "pseudo" RC of T = 1 time unit for 3 f_a-cycles and 5 f_b-cycles. The record is "clipped" at q = −1 (unclipped), −0.75, 0 and +0.9 amplitude units, as shown. (a) Fourier transforms for a record length of 100 time units sampled at 0.05 time units. Some of the harmonics $n_a f_a + n_b f_b$ are identified. (bottom) At frequencies below 1 cycle the spectrum consists of (i) HB frequencies down to $5f_a - 3f_b$ = 0.25 cycles, and (ii) harmonics 1, 2, . . . , 20 of the RC frequency T^{-1} = 0.05 cycles. The pseudo RC associated with T^{-1} = 0.99 cycles is limited to severe clipping of short record lengths, −2.5 < t < 2.5.
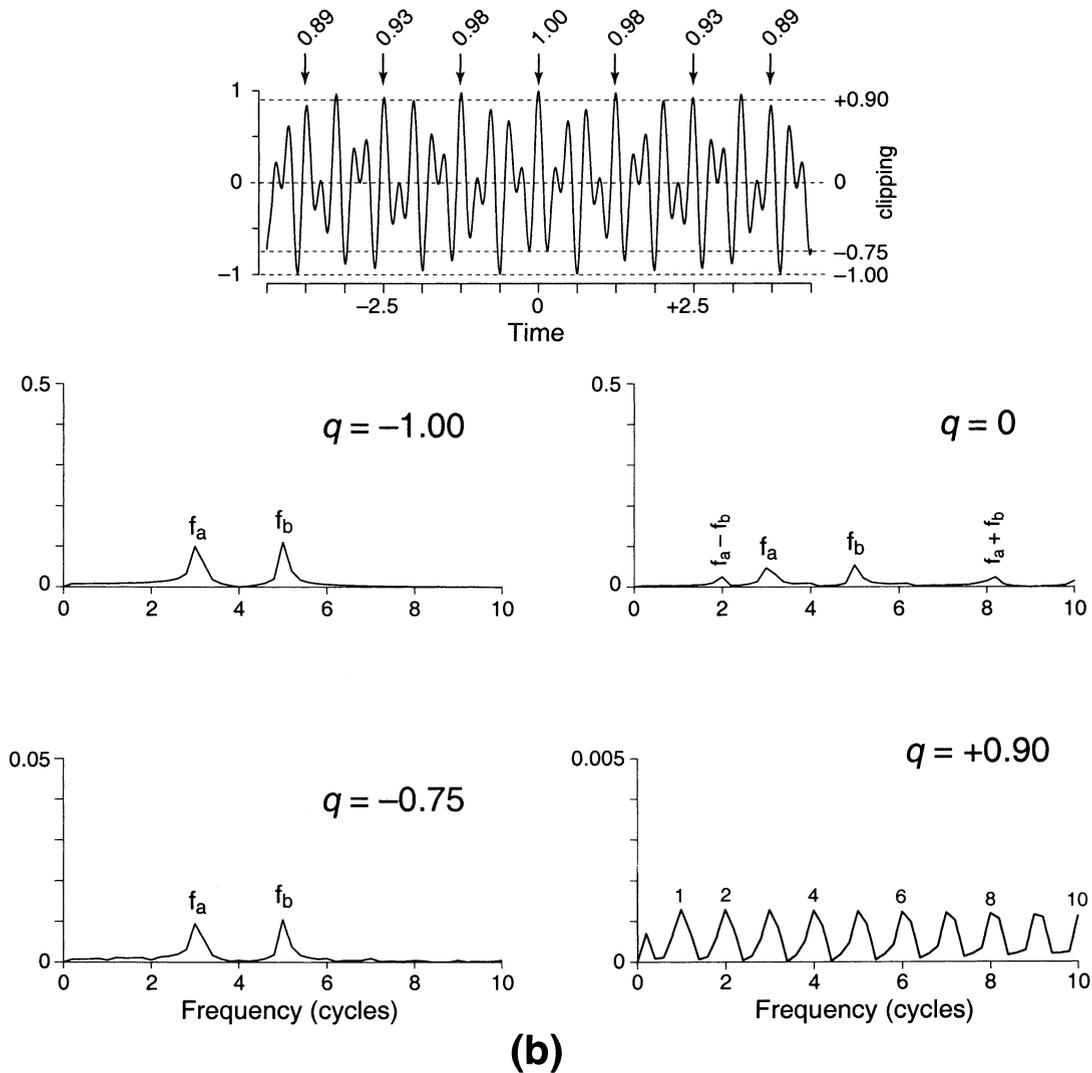
FIG. 4. (*Continued*)

issue is confused because KW uses the language of RC events, but with regard to the millennial variability KW (2000) come up with a period of 1795.26 yr that turns out to be the harmonic beat frequency

$$\delta f_{KW} = -f_{31} + 6f_4 + 6f_5 = 1/1795.26 \text{ yr} \quad (6.1)$$

from a triple interaction between lunar perigee, lunar nodes, and the anomalistic year. This can be written in terms of the four fundamental frequencies:

$$\delta f_{KW} = -f_3 + 6f_4 + 6f_5 + f_6 = 1/1795.26 \text{ yr.} \quad (6.2)$$

We omit the perihelion f_6 term and define an "adjusted KW frequency[1]"

---

[1] David Cartwright (2000, personal communication) has pointed out that it is preferable to follow KW and use the anomalistic year $f_{31} = f_3 - f_6$ instead of the tropical year f_3, because it directly specifies the passage of perihelion.

$$\delta f_{AKW} = -f_3 + 6f_4 + 6f_5 = 1/1963.6 \text{ yr.} \quad (6.3)$$

We have searched all $(21)^4$ cases for which n_2, n_3, n_4, and $n5$ have values from -10 to $+10$ for $\delta f < 0.001$ cpy. The only solutions are $\{0, 0, 0, 0\}$ and the above combination of $\{0, -1, 6, 6\}$. The KW cycle is remarkable for involving relatively low harmonics. Keeling and Whorf (2000) note that this 0.5702 cpky line lies within a broad peak 0.4–0.7 cpky found in glacial-Holocene petrologic events (Fig. 1). A second peak is centered at 0.21 cpky (KW have a special argument for a 0.215 cpky frequency). We refer here to a suggestion by Wunsch (2000) that a sharp line at 0.689 cpky (1452 yr) reported by Mayewski et al. (1997) is an alias associated with sampling at multiple intervals of the "calendar year" of exactly 365 days.

We now consider other possible HB frequencies. The combinations yielding cpky frequencies with moderate

TABLE 1. Tidal constituents. Periods are in days and tropical kiloyears; frequencies in cpy. Tropical month is sometime called "sidereal" month. The perihelion term is not ordinarily among the tidal constituents but is included in the Doodson expansion. The last three constituents are referred to as the Milankovich terms.

Day	1 d	$f_1 = 365.24219879$ cpy
Tropical month s	27.321582	$f_2 = 13.368267$
Tropical year h	365.24219879	$f_3 = 1$
Lunar perigean p	3231.49562	$f_4 = 0.113026$ (8.85 yr)
Lunar nodes–N	6798.32182	$f_5 = 0.053725$ (18.61 yr)
Perihelion p_s	20.94 ky	$f_6 = 4.7755 \times 10^{-5}$
Precession	19, 23	
Obliquity	41	
Eccentricity	95, 100, 213	

TABLE 2. Certain derived tidal constituents. Periods in days, frequencies in cycles per tropical year.

Tropical month	27.321582 day	$f_2 = 13.368267$ cpy
Nodical month	27.212220	$f_{21} = f_2 + f_5 = 13.421992$
Anomalistic month	27.554551	$f_{22} = f_2 - f_4 = 13.255240$
Synodic month	29.530589	$f_{23} = f_2 - f_3 = 12.368267$
Tropical year	365.24219879	$f_3 = 1$
Anomalistic year	365.25964134	$f_{31} = f_3 - f_6 = 0.999952$
Evectional year	411.786	$f_{32} = f_3 - f_4 = 0.886971$

harmonics is very limited (Table 4). The "Cartwright frequency" is outstanding in involving only two frequencies, f_4 and f_5 (their ratio is close to 1/2). For completeness, we include the Saros and metonic RC periods, though the high values of $n\epsilon$ are not favorable for the generation of low HB frequencies. For doublet interaction, a small value of $\delta f/f \approx n\epsilon$ is favorable to form low frequencies. We suggest

$$\text{PF} = (\delta f/f_{\min}) \sum_i |n_i| \qquad (6.4)$$

as a suitable "penalty function" (small is good), where $f_{\min}$ is the lower interacting frequency, and $\Sigma_i |n_i| = p$ is the power required to produce the nonlinearities [Eq. (4.10)]. For the adjusted KW (AKW) interaction $p = 13$ and PF = (0.509/53.7) 13 = 0.12.

However the orbital [Kepler–Newton (KN)] nonlinearities provide certain harmonics as input into the terrestrial [Navier–Stokes (NS)] nonlinearities. These "derived" constituents may be more efficient (e.g., smaller p) generators of low HB frequencies than the fundamental six constituents. Note that the strength of harmonic $2f_2$ (the fortnightly tide) exceeds the fundamental monthly tide f_2 (Fig. 3); in that spirit we surmise that KN nonlinearities have produced harmonics $2f_4$ and $3f_5$, in which case

$$\delta f_{\text{AKW}} = -f_3 + 3(2f_4) + 2(3f_5) \qquad (6.5)$$

and $p = 6$ (as confirmed by a numerical experiment, not shown). From Eqs. (6.1) and (6.2), the derived anomalistic year $f_{31} = f_3 - f_1$ yields $p = 13$ as compared to $p = 14$ for the tropical year f_3. The Saros cycle involves two derived constituents, the nodical and the synodic months (Table 2).

We need a systematic way to evaluate HB frequencies based on a suitable list of derived constituents.

7. The Doodson climate vector

We define the tide vectors:

$$\mathbf{f}^{\text{TIDE}} = \{f_1, f_2, f_3, f_4, f_5, f_6\}, \qquad (7.1)$$

consisting of the six fundamental tidal frequencies defined in Table 1. For the truncated vector $\{f_3, f_4, f_5\}$ we previously found that only the KW vector gave sub-cpky solutions:

$$\mathbf{n}_{\text{KW}} \cdot \mathbf{f}^{\text{TIDE}} = \{-1, 6, 6\} \cdot \{f_3, f_4, f_5\} = 0.51 \text{ cpky}.$$

The KN dynamics are associated with nonlinearities that produce harmonics of the fundamental tidal frequencies. Cartwright and Tayler (1971) and Cartwright and Edden (1975) list 484 terms whose amplitudes exceed 10^{-4} times the lunar equilibrium amplitude

$$K_2 = 0.358378 \text{ m.} \qquad (7.2)$$

The associated "Doodson frequencies" can be written

$$f_j^D = \mathbf{n}_j \cdot \mathbf{f}^{\text{TIDE}}, \qquad A_j > 10^{-4} K_2, \qquad j = 1, 2, \ldots 484,$$

where

$$\mathbf{n}_j = \{n_{j1}, n_{j2}, \ldots, n_{j6}\} \qquad (7.3)$$

are the "Doodson vectors." The largest amplitude is for M_2, namely, $\mathbf{n} = \{2, -2, 0, 0, 0, 0\}$: and $A = 0.908$. We wish to use the Doodson frequencies (rather than the tide frequencies) as our basis frequencies for generating HB frequencies. We define the Doodson matrix as

$$\mathbf{D} = \begin{bmatrix} n_{1,1} & n_{1,2} & \cdots & n_{1,6} \\ n_{2,1} & n_{2,2} & \cdots & n_{2,6} \\ \vdots & \vdots & \cdots & \vdots \\ n_{484,1} & n_{484,2} & \cdots & n_{484,6} \end{bmatrix}. \qquad (7.4)$$

We search for harmonics of the Doodson frequencies for which

$$F = \mathbf{m} \cdot \mathbf{f}^D = \mathbf{mD} \cdot \mathbf{f}^{\text{TIDE}} < 1 \text{ cpky}, \qquad (7.5)$$

where

$$\mathbf{m} = \{m_1, m_2, \ldots, m_{484}\} \qquad (7.6)$$

is the "millennial vector." As previously, let $p = \Sigma |m_j|$ designate the order of the polynomial required to generate the harmonics. For $p = 1$, the Fs are simply the $J = 484$ Doodson frequencies f^D, and none are lower than 1 cpky. The case $p = 2$, is essentially a search for all possible $\frac{1}{2}J(J + 1)$ differences between Doodson frequencies, but again none fulfill condition (7.5). The same is true for $p = 3$. For $p = 4$ and 484 frequencies,

TABLE 3. Parameters evaluated from Eq. (4.11). The column marked * is associated with the Saros cycle.

n_a	1	6	10	47	176	223*	493	4518
n_b	1	7	11	51	191	242*	535	4904
$n\varepsilon$	0.08	0.4	0.1	0.004	0.005	0.001*	0.004	0.0005

there are 162 combinations (out of $484^4 = 5 \times 10^{10}$) that do satisfy the imposed cpky frequency limit. In only one case,

$$\mathbf{m} \cdot \mathbf{D} = \{1, 2, -1\} \begin{bmatrix} 0 & 0 & 1 & 0 & 0 & 0 \\ 1 & -2 & 0 & -1 & -3 & 0 \\ 2 & -4 & 0 & 4 & 0 & 0 \end{bmatrix}$$

$$= \{0, 0, 1, -6, -6, 0\} \qquad (7.7)$$

do we recover the adjusted KW frequency. There are 83 cases leading to the KW case $\{0, 0, 1, -6, -6, 1\}$ and 78 cases leading to $\{0, 0, 1, -6, -6, -1\}$. There are no other solutions for $p = 4$. The three cases $n_6 = +1, 0, -1$ are associated with values $(2.6, 1.5, 9.1)$ 10^{-15} mm^4.

This leads to a number of interesting results: (i) using the complete set of 484 Doodson vectors rather than the 6 primary tidal frequencies reduces the required nonlinearity from $p = 13$ to $p = 4$. (ii) Some of the interacting constituents include the strong semidiurnal and diurnal frequencies [see Eq. (7.5)], and (iii) these include diurnal and annual frequencies with significant radiational components.

This is as far as (perhaps further than) we shall want to go with tidal numerics. The complexity argues for an analysis in the time domain, especially since some of the frequencies will drift over the time span considered here.

8. Secular change

So far we have dealt with incommensurate frequencies. Secular changes in the orbits will bring some tidal frequencies into occasional resonance. Halley (1695) discovered an *acceleration* in the lunar orbit by 10 arcs century^{-2}. The most accurate estimate now comes from lunar laser ranging, using the retroreflector placed on the Moon in 1969 during the Apollo missions. The Moon's distance is increasing at a rate of 3.82 ± 0.7 cm yr^{-1} (Dickey et al. 1994; Bills and Ray 1999). This is attributed to a transfer from Earth's spin momentum to the Moon's orbit momentum associated with the dissipation of tidal energy. With $a = 384\,402$ km for the semimajor axis, $(1/a) \, da/dt = 1.00 \times 10^{-10}$ yr^{-1}. From Kepler's law $f_1^2 a^3 = $ constant, we find $(1/f_1) \, df_1/dt = -3/2(1/a) \, da/dt$, and so

$$\dot{f}_1 \equiv df_1/dt = -(0.00200 \pm 2\%) \text{ cycles ky}^{-2}. \quad (8.1)$$

The lunar orbital angular velocity of 13.4 cpy decreases by 0.002 cpy every million years.

Referring to the metonic cycle (Table 4),

$$\delta f = 19 f_1 - 254 f_2 = -2.93 \text{ cpky} \qquad (8.2)$$

and so a negative $\dot{f}_1$ will make it even more negative in the future. Looking backward, δf was zero at a time

$$-\frac{\delta f}{19 \dot{f}_1} = -77 \text{ ky}. \qquad (8.3)$$

The zero-crossing event is portrayed in the time domain in Fig. 6. If the metonic cycle could be isolated in the record, a trace of the zero crossing would be a welcome test of whether tidal dissipation has remained at the present rate for 100 000 yr.

9. A numerical experiment

We wish to gain some further insight by applying the nonlinear filters $x^p(t)$ and $C_q[x(t)]$ on a time series $x(t)$ that bears resemblance to the actual tides. For $p = 1$ and q sufficiently negative we are back to the unfiltered time series.

We use the development in the time domain of the tidal spherical harmonics $c_n^m(\lambda, \phi; t)$ by Cartwright and Tayler (1971) and Cartwright and Edden (1973). The traditional harmonic expansion is deliberately avoided. An early version of the Cartwright expansion is the basis of the response method of tidal prediction (Munk and Cartwright 1966).

We arbitrarily chose the location of Honolulu, Hawaii (21.3°N, 202.2°W), to compute the equilibrium tide at 10-min intervals for a period of 275 601 yr. This included all of the f_1 to f_5 constituents; the perihelion term in f_6 was omitted (thus avoiding perihelion splitting). Terdiurnal tides $3 f_1$ are included, so that the highest linear frequency is 3 cpday. When raised to the fifth power this yields frequencies up to 15 cpday, which are adequately sampled at 10-min intervals.

A Hanning filter with a 2-day window, subsampled at daily intervals, was used to find filter these 10-min values. The record of 275 601 yr of daily averages was then broken into 5 overlapping segments of 91 867 yr. A sample of the record is shown in Fig. 7.

For a segment length of 91 867 yr the frequency resolution is roughly 0.01 cpky and the KW frequency of about 0.5 cpky is well resolved. Figure 8 shows the spectrum over the lower ranges of frequency that are of interest here. The regressional term f_5 is prominent. Some of the terms listed in Table 4 can be recognized. The Cartwright term $f_4 - 2f_5 = 5.6$ cpky (179 yr) first
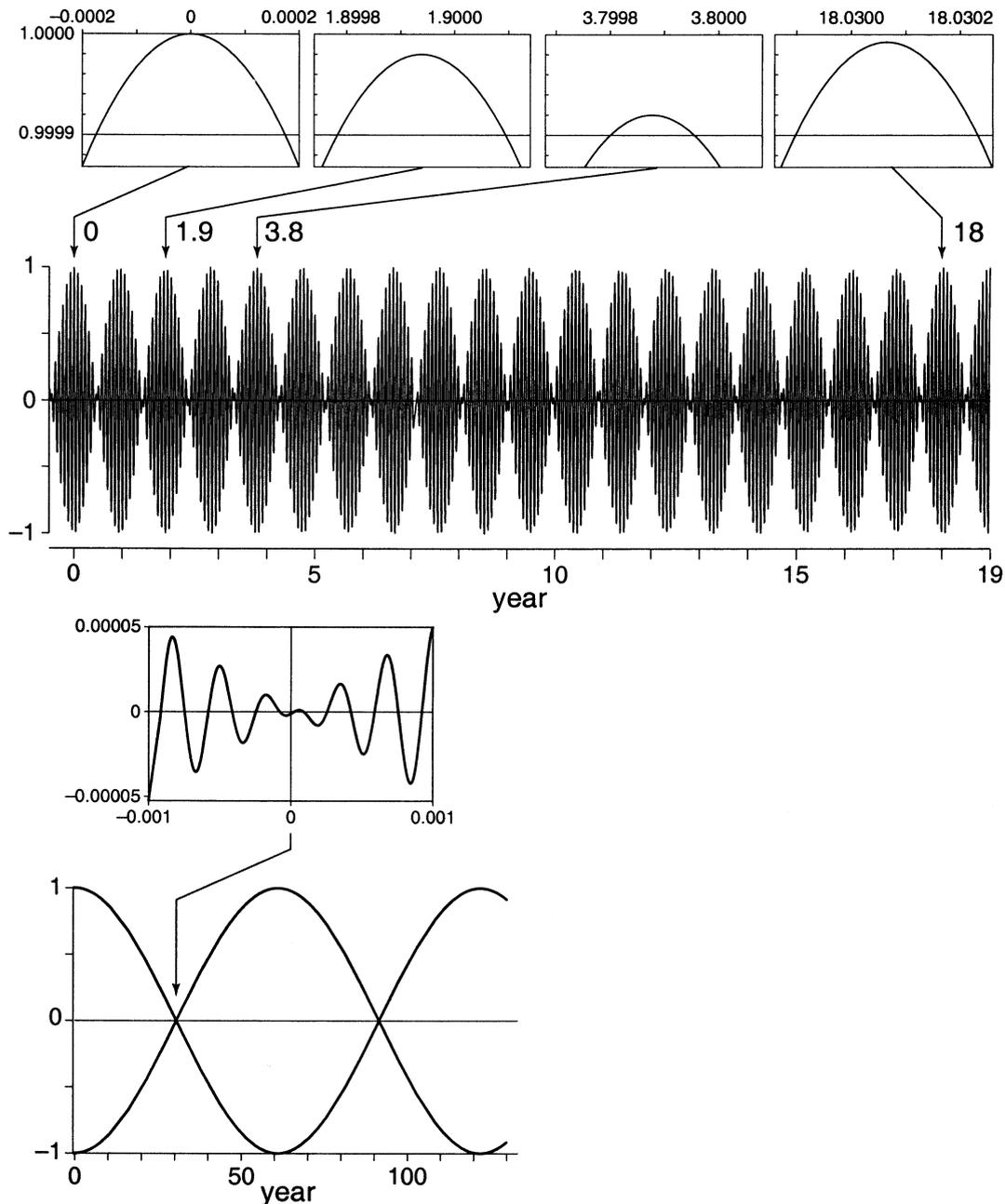
FIG. 5. Generation of the Saros RC period of 18.03 yr. Constructive interference between the nodical and synodic oscillations result in high values at 0.95-yr intervals. Staring with perfect overlap with unit amplitude, a near overlap of 0.9999 is exceeded 3 times in the first 20 yr, and a value of 0.99999 only once, after 18.03 yr (upper panel), showing the detailed oscillation over an interval of 0.0004 yr, or about 3½ h. Bottom panels show the envelope of a beat frequency of 1 cycle in 122 yr between the 223d harmonic of the nodical month and the 242d harmonic of the synodic month.

appears in the squared record, and its harmonic in the cubed record.

To detect features in the millennial band required further filtering. The side bands of the f_5 peak caused by the discontinuities of the record segments obliterated all low frequencies in the raw analysis (not shown). The spectral level at the low frequencies was reduced by 6

orders of magnitude by applying a Hanning data window to each segment, but at the expense of a reduced resolution (widening of the f_4 peak). Without such severe tapering the peaks associated with HB frequencies around 1 cpky could not be detected.

The KW is prominent at $p \geq 4$, as expected. Using a test signal we have determined that the apparent broad-

TABLE 4. The HB frequencies $\delta f = n_2 f_2 + \cdots + n_5 f_5$ (cpky) for stated values of n_i. The top four lines give conventional tidal frequencies. The next five lines give differences between frequency pairs, so chosen to yield the lowest δf for the smallest possible $\Sigma|n_i|$. The combination $n_4 = 10$, $n_5 = -21$ is featured by Cartwright (1974). The only efficient triplet is the adjusted KW (2000) combinations. Any lower frequencies require very high harmonics. The "penalty function" (PF) is defined in Eq. (6.4).

n_2	n_3	n_4	n_5	δf cpky	PF		$1/\delta f$
1	0	0	0	13 368		Tropical month	0.0748 yr
0	1	0	0	1000		Tropical year	1
0	0	1	0	113		Lunar perigee	8.85
0	0	0	1	53.7		Lunar nodes	18.61
19	−242	0	−223	16.32	147	Saros	61.3
0	0	1	−2	5.58	0.7		179
0	1	−5	−8	5.07	1.3		197
0	0	−9	19	3.55	1.9		282
19	−254	0	0	−2.93	0.8	Metonic	341.3
0	0	10	−21	2.03	1.2	Cartwright	493
0	−13	115	0	−1.98	2.2		503
−1	14	−7	3	1.73	0.8		579
0	−1	6	6	0.509	0.12	KW adjusted	1964
1	−11	−20	−2	0.292	0.18		3422
2	−28	5	13	0.094	0.08		10 617

ening is consistent with the expected effects of windowing; there is no evidence here for anything but a single line (and no perihelion splitting since f_6 was omitted from the generated time series). A number of spectral lines at and above 1 cpky have not been identified.

The lower panel shows the spectrum clipped at various levels (see Fig. 7). Only the f_5 peak is noticeable; rather disappointingly there is no evidence for any of the RC terms, even at severe clipping. We suspect some of the RC frequencies would show up in an analysis of relatively short record lengths, as indicated in Fig. 4.

Finally, we make an estimate of the energy at the KW frequencies. We previously reported the numerical values of the three spectral lines corresponding to $n_6 = +1, 0, -1$, using Cartwright and Edden numerology. From these we estimate

$$\left[\frac{1}{8}(1.2 + 0.7 + 4.3)10^{-5}\right]^{1/4} = 0.05 \text{ mm} \quad (9.1)$$

of equivalent tidal amplitude (the factor 1/8 comes from the fact that for nonlinear combination of two frequencies 1/2 of the amplitude goes to the sum frequency and 1/2 goes to the difference frequency, and this happens 3 times for the fourth power interaction). The energy in the spectral peak in Fig. 8 yields an amplitude of 0.04 mm.

10. Discussion

Keeling and Whorf (1997, 2000) propose that millennial climate variability is associated with tidal forcing. There is indeed a resemblance between the measured spectrum (Fig. 1) and the spectrum of the tide potential as seen through a nonlinear polynomial filter (Fig. 8). But the recorded band structure (rather than line structure) is more consistent with nonorbital generation, such as instabilities in the ocean–atmosphere dynamics, a variable solar radiation, etc.

Assuming orbital forcing, one needs to take into account that the millennial frequency is 5 octaves above the highest Milankovitch frequencies, and 5 octaves below the lowest tidal frequencies. To penetrate the gap one needs high Milankovitch harmonics or high tidal subharmonics. The KW proposal is for nonlinear generation of the tidal subharmonics.

We consider two processes by which tidal orbits can produce low-frequency forcing. Keeling and Whorf refer to the occurrence of repeat coincidence in the orbital parameters. Eclipse "cycles" are associated with such RC events. Extreme high tides occur at long intervals, and the more extreme the tide the longer the interval. The problem here is that RC events are of very short duration (like eclipses). Beat frequencies between neighboring harmonics persist over the time interval of the interference pattern, and are a more likely cause of climate variability.

Given sufficiently high nonlinearities (hard clipping or high-power polynomials), the many harmonics generated are sufficiently densely distributed that there will be some combinations forming low difference frequencies. This is a consequence of Dirichlet's Theorem (Hardy and Wright 1960, p. 375); it remains to be seen whether the penalty function (6.4) associated with the orbital constants of the solar system differs from what is expected from an equivalent set of random numbers.

In their earlier paper, KW (1997) featured decadal and centennial repeat coincidences. We suggest that harmonic beat frequencies are more likely candidates (Table 4); $f_4 - 2f_5$ (178 yr) and its harmonic $2(f_4 - 2f_5)$ (89 yr) are particularly prominent in the numerical experiments (Fig. 8). Any supporting evidence from the
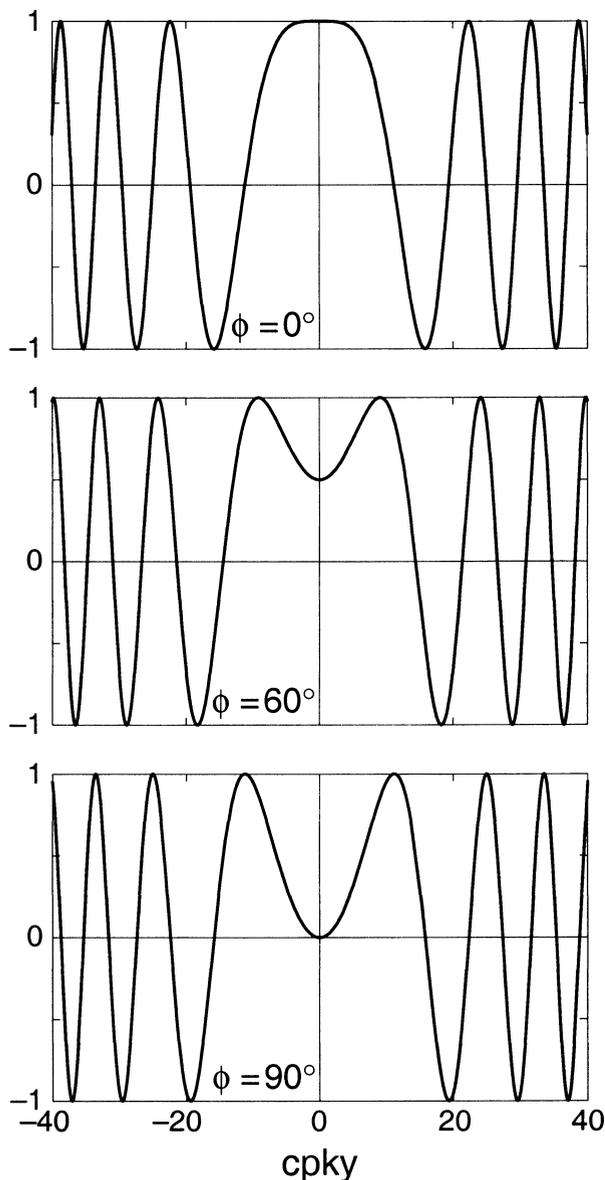
FIG. 6. Zero-crossing events $\cos(2\pi n_1 \dot{f}_1 t^2 - \phi)$ for $n_1 = 1$ and $f_1 = -2 \times 10^{-3}$ cycles ky^{-2} associated with tidal friction. The transient duration is roughly $40\, n_1$ ky^{-1}.

FIG. 7. Equilibrium tide for Hawaii (21.3°N, 202.2°W) for (top) a month and (bottom) 30 yr. Monthly, annual, and regressional variability can be seen.

climate record would strengthen the KW case for tidal generation of millennial variability.

From orbital considerations, KW incisively argue for a 1795-yr period, and this corresponds to the combination $(-f_3 + 6f_4 + 6f_5)$ of the annual, lunar perigee and nodal frequencies. Our (somewhat brute force) search through the frequency and time domains reveals no other combination of comparably low harmonics to yield millennial frequencies. Even so, this requires the nonlinear fourth power interaction of tidal constituents. The equivalent tidal amplitude of the millennial term is estimated at 0.04 mm. It is difficult to suppose that this is of sufficient amplitude, and associated with sufficient
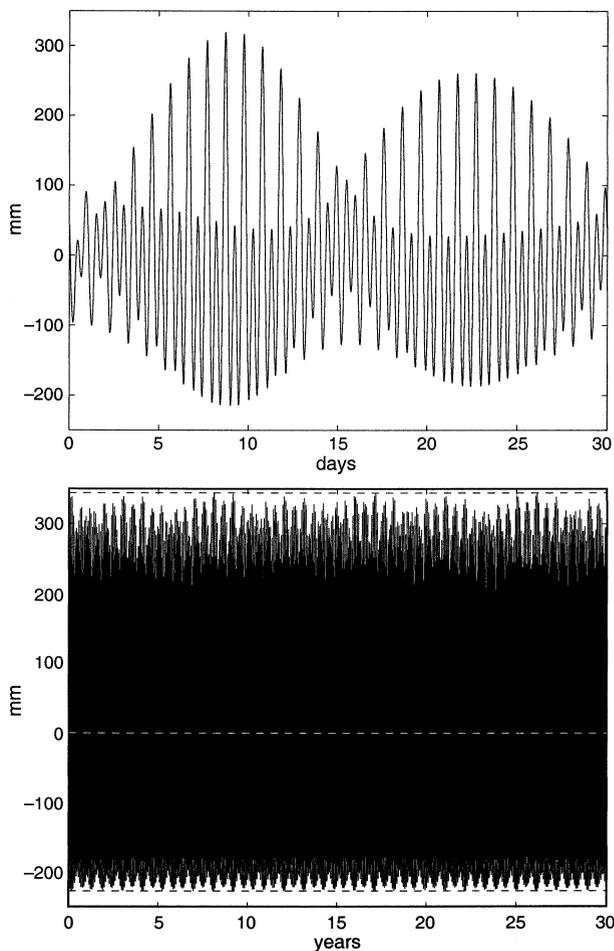
climate perturbation, to account for the millennial variability. In conclusion, we favor processes with millennial time constants (not yet identified) inherent in ocean–atmosphere dynamics as the source of the millennial climate variability; millennial variability in solar radiation (not yet discovered) is a possibility. But low beat frequencies between tidal harmonics (rather than repeat coincidence, the traditional view) cannot be ruled out by any evidence known to us; if indeed these are a factor, the low amplitude notwithstanding, then the {−1, 6, 6} combination proposed by KW is the most likely candidate.
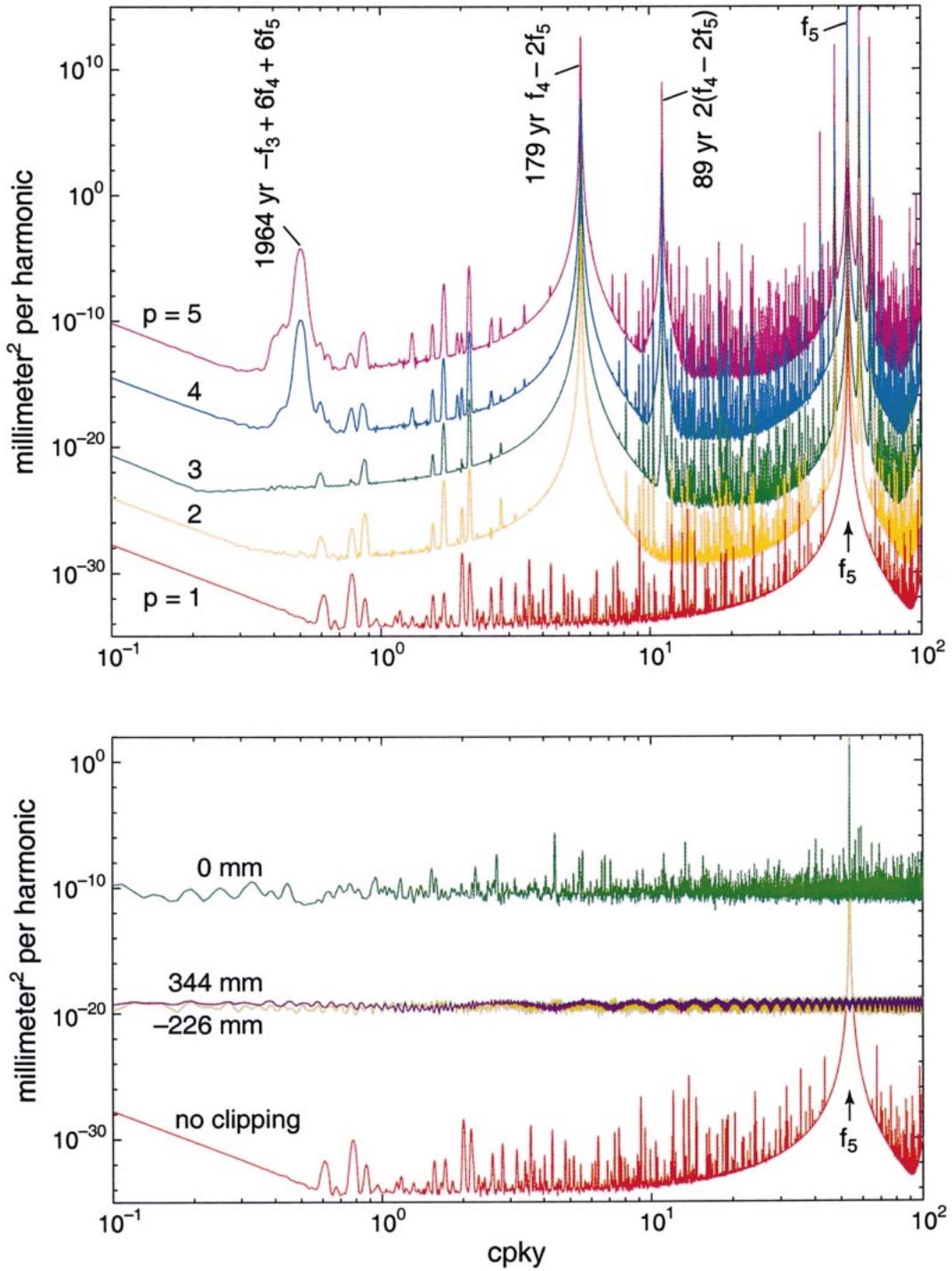
FIG. 8. (top) Spectra of the equilibrium time series raised to powers $p = 1$ to 5 and (bottom) clipped as indicated. The lowest spectra (linear, no clipping) are identical. Lunar regression (f_5) appears in the linear record. A HB frequency $f_4 - 2f_5$ is generated at $p = 2$, and twice that frequency at $p = 3$. The KW line $-f_3 + 6f_4 + 6f_5$ is generated for $p = 4$. Clipping does not generate any identifiable HB events.

University of Colorado. His computations were performed at the National Center for Atmospheric Research under support of the National Science Foundation. Breck Betts and Andrea Santos assisted in the preparation of the manuscript.

APPENDIX A

Spectral Lines and the Continuum

Let

$$x(t) = \sum_n A_n \cos(2\pi f_n t + \alpha_n) + y(t) \quad \text{(A.1)}$$

designate the tidal response to orbital forcing at frequencies f_n plus the residual response. The associated power spectrum has the two terms

$$X(f) = A_n^2 \delta(f - f_n) + Y(f) \quad \text{(A.2)}$$

corresponding to the discrete lines at the orbital frequencies plus the continuum spectrum. Here $Y(f)$ is the power density (mm^2 cpy^{-1}) represented by the gray area in the Fig. 2; the vertical lines are to be interpreted as mm^2 of response to orbital forcing.

In the early days of tidal analysis it was assumed that the observed tidal records consisted entirely of the line spectrum associated with orbital forcing. Not until the advent of modern computers was it possible to resolve the intertidal continuum underlying the line spectrum (Munk and Cartwright 1966). The continuum spectrum was found to be red, rising from 0.3 mm^2 cpy^{-1} at diurnal frequencies to 1000 mm^2 cpy^{-1} at decadal frequencies. Accordingly in the frequency band covering months to days the continuum variance is of the order

$$\int_{10 \text{ cpy}}^{300 \text{ cpy}} Y(f)\, df \approx 10^2 \text{ mm}^2 \quad \text{(A.3)}$$

and negligible as compared to a tidal variance of order 10^5 mm^2. In the frequency band from decades to years,

$$\int_{0.1 \text{ cpy}}^{10 \text{ cpy}} Y(f)\, df \approx 10^3 \text{ mm}^2 \quad \text{(A.4)}$$

exceeds the long-period tidal variance of 10^2 mm^2. Accordingly, most of the variance above 1 cpy is associated with the orbital line spectrum, whereas the continuum dominates over lower frequencies.

The situation is not clear for the Milankovitch range of frequencies.

APPENDIX B

Gravitational and Radiational Forcing

The response to the orbital forcing is generally reckoned in terms of elevation for the traditional tidal forces, and in terms of temperature and other climate proxies for the Milankovitch forcing. Here we compare gravitational and radiational solar forcing in terms of equivalent sea level. The equilibrium response to a gravitational potential V is

$$\eta = \frac{V}{g} = \frac{GM}{gR} = 0.16 \text{ m} \quad \text{(B.1)}$$

for a solar mass M and distance R. The solar "constant" equals

$$C = \frac{S}{4\pi R^2} = 1360 \text{ W m}^{-2}, \quad \text{(B.2)}$$

where S is the solar radiation. The Earth (radius a) intercepts $\pi a^2 C$ W that, when distributed over the entire surface $4\pi a^2$ (night and day), yield an average power (the insolation) $I = 1/4\ C$. At any given point the insolation can be expanded into the mean value I plus variable terms of amplitude δI, much like the expansion of the tidal potential (Munk and Cartwright 1966).

The temperature θ of a unit water column of depth h will increase according to $d\theta/dt = I/(\rho h s)$. Thermal expansion will lead to a rise in sea level

$$d\eta/dt = kI,$$
$$k = \alpha/(\rho s) = 2.5 \times 10^{-11} \text{ m}^3 \text{ J}^{-1}, \quad \text{(B.3)}$$

where $\rho = 10^3$ kg m^{-3}, $\alpha = -(1/\rho)d\rho/d\theta = 10^{-4}$ °C^{-1} is the thermal expansion, and $s = 4000$ J (kg °C)$^{-1}$ the specific heat. Depth of heating enters only to the extent that thermal expansion is a function of temperature. A *steady* radiation over a period of 1 yr raises sea level by $3.15 \times 10^7\ d\eta/dt = 0.2$ m, which is of the same order as (B.1). The annual *perturbation* in sea level is a small (but similar) fraction of these two numbers and can be derived by a suitable spherical harmonic expansion (Munk and Cartwright 1966).

REFERENCES

Alley, R. B., and P. U. Clark, 1999: The deglaciation of the northern hemisphere: A global perspective. *Ann. Rev. Earth Planet Sci.*, **27,** 149–182.

Berger, W. H., 1999: The 100-kyr ice-age cycle: Internal oscillation or inclinational forcing? *J. Earth Sci.*, **88,** 305–316.

Bills, B., and R. D. Ray, 1999: Lunar orbital evolution: A synthesis of recent results. *Geophys., Res. Lett.*, **26,** 3045–3048.

Bond, G., and Coauthors, 1997: A pervasive millenial-scale cycle in North Atlantic holocene and glacial climates. *Science,* **278,** 1257–1266.

——, W. Showers, M. Eliot, M. Evans, R. Lotti, I. Hajdas, G. Bonani, and S. Johnson, 1999: *Mechanism of Global Climate Change at Millenial Time Scales. Geophys. Monogr.*, No. 112, Amer. Geophys. Union, 394 pp.

Cartwright, D. E., 1974: Years of peak astronomical tides. *Nature,* **248,** 656–657.

——, and R. J. Tayler, 1971: New computations of the tide-generating potential. *Geophys. J. Roy. Astron. Soc.,* **23,** 45–74.

——, and A. C. Edden, 1973: Corrected tables of tidal harmonics. *Geophys. J. Roy. Astron. Soc.,* **33,** 253–264.

Cerveny, R. S., and J. A. Shaffer, 2001: The moon and El Niño. *Geophys. Res. Lett.,* **28,** 25–28.

Dickey, J. O., and Coauthors, 1994: Lunar laser ranging: A continuing legacy of the Apollo program. *Science,* **265,** 482–490.

Doodson, A. T., 1921: The harmonic development of the tide-generating potential. *Proc. Roy. Soc. London,* **100A,** 305–329.

Garrett, C. J. R., 1979: Mixing in the ocean interior. *Dyn. Atmos. Oceans,* **3,** 239–265.

Ghil, M., and R. Vautard, 1991: Interdecadal oscillations and the warming trend in global temperatures. *Nature,* **350,** 324–327.

Grootes, P. M., and M. Stuiver, 1997: Oxygen 18/16 variability in Greenland snow and ice with 10^3- to 10^5-year time resolution. *J. Geophys. Res.,* **102,** 26 455–26 470.

Halley, E., 1695: Some account of the ancient state of the city of Palmyra, with short remarks upon the inscriptions found there. *Philos. Trans. Roy. Soc. London,* **19,** 160–175.

Hardy, G. H., and E. M. Wright, 1960: *An Introduction to the Theory of Numbers.* 4th ed. Clarendon Press, 421 pp.

Keeling, C. D., and T. P. Whorf, 1997: Possible forcing of global temperature by oceanic tides. *Proc. Natl. Acad. Sci.,* **94,** 8321–8328.

——, and ——, 2000: The 1800-year oceanic tidal cycle: A possible cause of rapid climate change. *Proc. Natl. Acad. Sci.,* **97,** 3814–3819.

Laskar, J., 1986: Secular terms of classical planetary theories using the results of general theory. *Astron. Astrophys.,* **157,** 59–70.

——, 1999: The limits of Earth orbital calculations for geological time-scale use. *Philos. Trans. Roy. Soc. London,* **357A,** 1735–1759.

Mann, M., and J. Park, 1994: Global-scale modes of surface temperature variability on interannual to century time scales. *J. Geophys. Res.,* **99,** 25 819–25 834.

Mayewski, P. A., L. D. Meeker, M. S. Twickler, S. Whitlow, Q. Yang, W. B. Lyons, and M. Prentice, 1997: Major features and forcing of high-latitude northern hemisphere atmospheric circulation using a 110 000-year-long glaciochemical series. *J. Geophys. Res.,* **102,** 26 345–26 366.

Milankovitch, M., 1941: *Kanon der Erdbestrahlung und seine Anwendung auf das Eiszeitproblem* (Canon of isolation and the Ice-Age problem). Special Publication, Vol. 132, Section of Mathematical and Natural Sciences, Vol. 33, Royal Serbian Academy, 484 pp. Translated by the Program for Scientific Translation, Jerusalem, Israel, Rep. TT 67-51410, 1969. [Available from U.S. Dept. of Commerce, Clearinghouse for Federal, Scientific and Technical Information, Springfield, VA 22151.]

Muller, R. A., and G. J. MacDonald, 2000: *Ice Ages and Astronomical Causes.* Springer-Verlag, 318 pp.

Munk, W. H., and E. C. Bullard, 1963: Patching the long-wave spectrum across the tides. *J. Geophys. Res.,* **68,** 3627–3634.

——, and D. E. Cartwright, 1966: Tidal spectroscopy and prediction. *Philos. Trans. Roy. Soc. London,* **259A,** 533–581.

——, and C. Wunsch, 1998: Abyssal Recipes II: Energetics of tidal and wind mixing. *Deep-Sea Res.,* **45,** 1977–2010.

Pettersson, O., 1914: Climatic variation in historic and prehistoric time. *Sven. Hydrogr.-Biol. Komm. Skr.,* **5,** 26 pp.

——, 1930: The tidal force. *Geogr. Ann.,* **12,** 261–322.

Quinn, T. R., S. Tremaine, and M. Duncan, 1991: A three million year integration of the Earth's orbit. *Astron. J.,* **101,** 2287–2305.

Shackleton, N. J., S. J. Crowhurst, G. P. Weedon, and J. Laskar, 1999: Astronomical calibration of Oligocene-Miocene time. *Philos. Trans. Roy. Soc. London,* **357A,** 1907–1929.

Wolfram, S., 1999: *The Mathematica Book.* 3d ed. Wolfram Media/Cambridge University Press, 1403 pp.

Wood, F. J., 1986: *Tidal Dynamics.* Reidel, 558 pp.

Wunsch, C., 2000: On sharp spectral lines in the climate record and the millennial peak. *Paleoceanography,* **15,** 417–424.